JCTC Journal of Chemical Theory and Computation

pubs.acs.org/JCTC Article

Wave Packet Control and Simulation Protocol for Entangled Two-Photon Absorption of Molecules

Bing Gu,* Daniel Keefer, and Shaul Mukamel*

Cite This: https://doi.org/10.1021/acs.jctc.1c00949 Read Online

ACCESS | Metrics & More | Article Recommendations

ABSTRACT: Quantum light spectroscopy, providing novel molecular information nonaccessible by classical light, necessitates new computational tools when applied to complex molecular systems. We introduce two computational protocols for the molecular nuclear wave packet dynamics interacting with an entangled photon pair to produce an entangled two-photon absorption signal. The first involves summing over transition pathways in a temporal grid defined by two light−matter interaction times accompanied by the field correlation functions of quantum light. The signal is obtained by averaging over the two time distribution characteristics of the entangled photon state. The other protocol involves a Schmidt decomposition of the entangled light and requires summing over the Schmidt modes. We demonstrate how photon entanglement can be used to control and manipulate the two-photon excited nuclear wave packets in a displaced harmonic oscillator model.

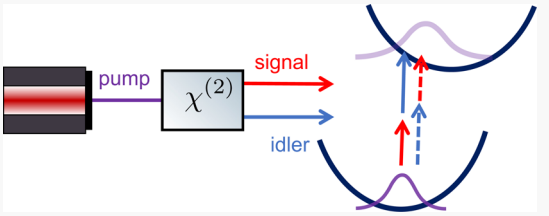

INTRODUCTION

Numerous novel spectroscopic techniques which exploit the variation of photon statistics upon interaction with matter are made possible by quantum light.[1,2] Such quantum spectroscopy has been demonstrated, both theoretically and experimentally, to be a powerful technique that can reveal molecular information not accessible by classical light[2] and can further enhance the signal-to-noise ratio and resolution beyond the classical limit.[3] The incoming photon statistics can be employed as a novel control knob for the optical response functions of matter,[4,5] in addition to the control knobs available to classical light.[6] Quantum optical effects such as the Hong−Ou−Mandel two-photon interference[7] can be used to generate signals which have no classical analogues.[8−10]

Entangled two-photon absorption (ETPA) has recently attracted considerable attention.[11−27] The extent to which the two-photon absorption rate can be enhanced by entangled light is under debate. While several ETPA experiments have been reported,[27,28] a recent theoretical analysis shows that ETPA events are below the detection level for typical molecular systems in realistic experimental setups.[11] In ETPA, a molecule is promoted from the ground state to an excited state by simultaneously absorbing two, degenerate or nondegenerate, photons. This technique drastically differs from the classical two-photon absorption. At low photon fluxes, it scales linearly, rather than quadratically with the pump photon intensity.[24,29] This is because the entangled photon pair generated by, for example, spontaneous parametric down-conversion[30−33] is created simultaneously and thus interacts with molecules at the same time. Furthermore, when a narrowband pump is utilized in the twin-photon generation, a strong frequency anticorrelation is exhibited, that is, detection of one photon reveals the frequency of its twin within a small uncertainty determined by the pump bandwidth (see Figure 1a). This energy−time entanglement can be used in spectros-

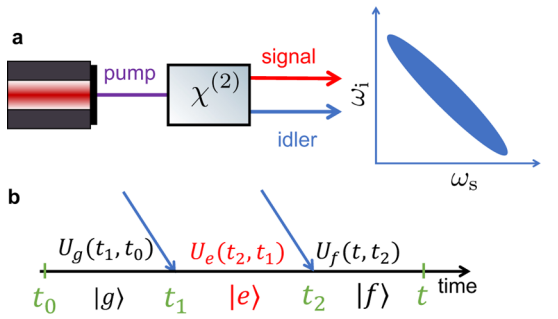

Figure 1. (a) Schematic of the SPDC process generating a frequency-anticorrelated photon pair. (b) Feynman diagram representing eq 11. $|g\rangle$, $|e\rangle$, and $|f\rangle$ represent the ground, intermediate, and final electronic states. $U_\alpha(t,t') = e^{i(T_n+V_\alpha(\mathbf{R}))(t-t')}$ is the free-molecule propagator on the αth PES. Between t_0 and t_1, the molecule remains in the ground state. The first photon, either signal or idler, brings the molecule to the intermediate state, launching nuclear dynamics on the associated PES.

Received: September 21, 2021

copy to manipulate the quantum interference among transition pathways, which have been shown to induce classically disallowed collective excitations,[34] and to probe classically dark bipolariton states.[21] As the ETPA signal depends on the entangled photon pair statistics, the biphoton joint spectral amplitude (JSA) can be used to optimize the two-photon excitation process, leading to quantum control by entangled light.[35] Early applications have focused on controlling the electronically excited state populations in model systems with frozen nuclear motion.[35] However, nuclear motions are responsible for reaction dynamics initiated by two-photon absorption, especially for molecules passing through conical intersections with strong vibrational−electronic (vibronic) coupling.

To fully describe the coupled electron−vibration−photonic dynamics, we develop a computational framework involving nuclear wave packet quantum dynamics interacting with quantum light. While the response to classical laser pulses can be obtained by solving the time-dependent Schrödinger equation, this is not the case for quantum light.

Our simulation protocol, based on time-dependent perturbation theory for the light−matter interaction, involves summing over all two-photon transition pathways in a two-dimensional temporal grid defined by the two interaction times with the entangled photon pair. Using a displaced harmonic oscillator model widely used to describe vibronic transitions,[36] we demonstrate how photon entanglement, a novel control knob not available for classical light, can be utilized to control the nuclear wave packet in electronically excited states. Three scenarios are examined, whereby the intermediate electronic state is resonant, off-resonant, and far-off-resonant with the incoming photons. We find that the two-photon-excited population is the largest for the resonant case. A linear dependence of the final-state population on the entanglement time is found for short entanglement times. This observation is rationalized by an analysis based on the sum-over-state expression. We further demonstrate that entanglement provides a useful control knob for the two-photon-excited wave packets. Modulating the entanglement time has the strongest effect on the shape of the created nuclear wave packet in the off-resonant case.

THEORY AND COMPUTATION

ETPA Signal. We consider a molecule−photon system described by the Hamiltonian ($\hbar = e = 4\pi\epsilon_0 = 1$)

$$H = H_{\mathrm{M}} + H_{\mathrm{R}} + H_{\mathrm{RM}} \tag{1}$$

The molecular Hamiltonian $H_{\mathrm{M}} = T_{\mathrm{n}} + H_{\mathrm{BO}}(\mathbf{R})$ represents the vibronic dynamics, where T_{n} is the nuclear kinetic energy operator, $H_{\mathrm{BO}}(\mathbf{R}) = \sum_\alpha V_\alpha(\mathbf{R})|\psi_\alpha(\mathbf{R})\rangle\langle\psi_\alpha(\mathbf{R})|$ is the adiabatic (Born−Oppenheimer) electronic Hamiltonian, with $V_\alpha(\mathbf{R})$ being the αth potential energy surface (PES). The radiation Hamiltonian

$$H_{\mathrm{R}} = \sum_{j=\mathrm{s,i}} \int_0^\infty \mathrm{d}\omega\ \hbar\omega\left(a_j^\dagger(\omega)a_j(\omega) + \frac{1}{2}\right) \tag{2}$$

represents two continua of photon modes, signal and idler, generated by a SPDC process; $H_{\mathrm{RM}} = \sum_j -\boldsymbol{\mu}\cdot\mathbf{E}_j(\mathbf{r})$ is the light−matter interaction in the electric dipole approximation, where $\mathbf{E}_j(\mathbf{r}) = \mathbf{E}_j^{(+)}(\mathbf{r}) + \mathbf{E}_j^{(-)}(\mathbf{r})$ and

$$\mathbf{E}_j^{(+)}(\mathbf{r}) = i\int_0^\infty \mathrm{d}\omega\ \mathcal{E}(\omega)\mathbf{e}_j a_j(\omega)\ \mathrm{e}^{-\mathrm{i}\mathbf{k}\cdot\mathbf{r}} \tag{3}$$

the electric field operator of the jth photon beam with polarization $\mathbf{e}_j$ at molecular location $\mathbf{r}$, and $\mathcal{E}(\omega) \equiv \sqrt{\frac{2\pi\omega}{cnA}}$ with the beam transversal area A, the refractive index n, and the speed of light c.

The joint electron−nuclear−photonic space is given by the tensor product of the electron−nuclear Hilbert space and the photon mode Fock space. The joint light−matter state is

$$|\Psi(t)\rangle = \sum_{\alpha,n} |\psi_\alpha(\mathbf{R})\rangle|\chi_{\alpha,\mathbf{n}}(t)\rangle|n(\omega)\cdots\rangle \tag{4}$$

where $|\psi_\alpha(\mathbf{R})\rangle$ is the adiabatic electronic state, $\chi_{\alpha,\mathbf{n}}(\mathbf{R},t)$ is the nuclear wave function at the αth electronic state, and the photon state is described in the occupation number representation $|\mathbf{n}\rangle \equiv |n(\omega)n(\omega')\cdots\rangle$. The initial state of the joint light−matter system is $|\psi_0(\mathbf{R})\rangle|\chi_0\rangle|\Phi_0\rangle$, where $|\Phi_0\rangle$ describes the quantum light.

The probability of arriving at the final electronic state $|\psi_f\rangle$ at time t is given by

$$\begin{aligned} P(t) &= \int \mathrm{d}\mathbf{R}\langle\Psi(t)||\psi_f(\mathbf{R}),\mathbf{R}\rangle\langle\psi_f(\mathbf{R}),\mathbf{R}|\otimes|0\rangle\langle 0||\Psi(t)\rangle \\ &= \int \mathrm{d}\mathbf{R}\,|\chi_f(\mathbf{R},t)|^2 \end{aligned} \tag{5}$$

where

$$\chi_f(\mathbf{R},t) = \langle\psi_f(\mathbf{R}),\mathbf{R}|\otimes\langle 0||\Psi(t)\rangle \tag{6}$$

is the nuclear wave function for the final electronic state created by the two-photon excitation process, where the photon modes are in the vacuum state $|0\rangle$. This is obtained by projecting the total state onto the final electronic state and the photon vacuum after the pump pulse $t > t_{\mathrm{p}}$.

The joint light−matter state at time t is obtained using time-dependent perturbation theory in the light−matter interaction. To second order, we have

$$\begin{aligned} |\tilde{\Psi}(t)\rangle = -\sum_{i,j}\int_{t_0}^{t}\mathrm{d}t_2\int_{t_0}^{t_2}\mathrm{d}t_1(\boldsymbol{\mu}(t_2)\cdot\mathbf{e}_j)(\boldsymbol{\mu}(t_1)\cdot\mathbf{e}_i)|\psi_0\rangle|\chi_0\rangle \\ E_j^{(+)}(t_2)E_i^{(+)}(t_1)|\Phi_0\rangle \end{aligned} \tag{7}$$

where $A(t) = U_0^\dagger(t)AU_0(t)$ is the operator A in the interaction picture of $H_0 = H_{\mathrm{M}} + H_{\mathrm{R}}$, and i, j label the beam. We consider two incoming beams and neglect the zero- (no interaction) and first-order (one-photon) processes in eq 7 as they do not contribute to the two-photon absorption. The dipole operator acts in the joint electron−nuclear space

$$\boldsymbol{\mu} = \sum_{\alpha\neq\beta}\int \mathrm{d}\mathbf{R}\langle\psi_\beta(\mathbf{R})|\boldsymbol{\mu}|\psi_\alpha(\mathbf{R})\rangle_{\mathbf{r}}|\psi_\beta(\mathbf{R}),\mathbf{R}\rangle\langle\psi_\alpha(\mathbf{R}),\mathbf{R}| \tag{8}$$

where α, β labels the electronic states and $\langle\cdots\rangle_{\mathbf{r}}$ refers to the integration over the electronic degrees of freedom. We further assume that the molecule has no permanent dipole moments so that $\alpha \neq \beta$.

Inserting eq 7 into eq 6 yields

https://doi.org/10.1021/acs.jctc.1c00949
J. Chem. Theory Comput. XXXX, XXX, XXX−XXX

$$\tilde{\chi}_f(\mathbf{R}, t) = -\sum_{i,j}\sum_{e}\int_{t_0}^{t} dt_2 \int_{t_0}^{t_2} dt_1\, V_{fe}^{(j)}(\mathbf{R}, t_2) V_{eg}^{(i)}(\mathbf{R}, t_1) \chi_0(\mathbf{R}) \Phi_{ji}(t_2, t_1) \quad (9)$$

where $V_{\beta\alpha}^{(j)}(\mathbf{R}) = \langle \psi_\beta(\mathbf{R})|\boldsymbol{\mu}\cdot\mathbf{e}_j|\psi_\alpha(\mathbf{R})\rangle_r$ is the transition dipole moment projected on the polarization of jth photon beam, e runs over all intermediate electronic surfaces, and

$$\Phi_{ji}(t_2, t_1) = \langle 0|E_j^{(+)}(t_2) E_i^{(+)}(t_1)|\Phi_0\rangle \quad (10)$$

is the entangled two-photon transition amplitude.

Transforming back to the Schrodinger picture, we obtain

$$\chi_f(\mathbf{R}, t) = -\sum_{i,j}\sum_{e}\int_{t_0}^{t} dt_2 \int_{t_0}^{t_2} dt_1 \xi(t_2, t_1)$$

$$\xi(t_2, t_1) \equiv U_f(t, t_2) V_{fe}^{(j)}(\mathbf{R}) U_e(t_2, t_1) V_{eg}^{(i)}(\mathbf{R}) U_g(t_1, t_0) \chi_0(\mathbf{R}) \Phi_{ji}(t_2, t_1) \quad (11)$$

where $U_\alpha(t,t') = e^{-i(T_n+V_\alpha(\mathbf{R}))(t-t')}$ describes the wave packet dynamics in αth PES. The wave packet $\xi(t_2, t_1)$ represents a single two-photon absorption event, with two light−matter interactions occurring at t_1 and t_2. This reduces to the $|g\rangle \rightarrow |f\rangle$ transition amplitude if the nuclear motion is frozen.

Using the Feynman diagram (Figure 1b) eq 11 can be interpreted as follows: The final nuclear wave packet at time t on the fth PES is given by a sum over all possible transition pathways. Each pathway contains two dipole interaction times t_1 and t_2, where the molecule undergoes a transition between electronic states. Between t_0 and t_1, the molecule remains at the ground state. At t_1, the molecule makes a transition to the eth electronic state, launching a nuclear wave packet dynamics until it interacts with the second photon at t_2, which brings it to the final f-PES. Nuclear dynamics then takes place between t_2 and the final time t on this PES. Each two-photon transition pathway depends on the two-photon transition amplitude $\Phi_{ji}(t_2,t_1)$, whose modulus squared gives the probability of detecting the i photon at time t_1 and j photon at t_2. The molecule thus serves as a photodetector.[37] The dependence of the ETPA signal on the photon statistics allows to control the two-photon-excited nuclear wave packet on the excited-state PES by shaping the two-photon wave function.

Energy−Time Entangled Light. The two-photon wave function is described by the JSA of the entangled photon pair. Here, we employ the twin-photon, signal and idler, state, generated by a type-II SPDC process[26,31,32]

$$|\Phi\rangle = \int_0^\infty\int_0^\infty d\omega_s\, d\omega_i\, J(\omega_s, \omega_i) a_s^\dagger(\omega_s) a_i^\dagger(\omega_i)|0\rangle \quad (12)$$

where the JSA $J(\omega_s, \omega_i)$ is the amplitude of detecting the signal photon with frequency ω_s and idler photon with frequency ω_i, and $a_j(\omega)(a_j^\dagger(\omega))$ annihilates (creates) a j photon with frequency ω, satisfying the boson commutation relation $[a_j(\omega), a_{j'}^\dagger(\omega')] = \delta_{jj'}\delta(\omega - \omega')$.

We focus on the frequency anticorrelation of the entangled photons and suppress the spatial degrees of freedom.[32,38] For a Gaussian pump with central frequency $\bar{\omega}_p$ and bandwidth σ_p, the JSA reads

$$J(\omega_1, \omega_2) = \mathcal{N} \exp\left(-\frac{(\omega_1 + \omega_2 - \bar{\omega}_p)^2}{4\sigma_p^2}\right) \mathrm{sinc}\left(\frac{\Delta k L}{2}\right) \quad (13)$$

where L is the crystal length, $\Delta k = k_s(\omega_s) + k_i(\omega_i) - k_p(\omega_s + \omega_i)$ is the wavenumber mismatch, $k_j = n_j(\omega_j)\omega_j/c$, $\mathcal{N}$ is the normalization factor ensuring $\iint d\omega_s\, d\omega_i |J(\omega_s,\omega_i)|^2 = 1$, and $\mathrm{sinc}(x) = \sin(x)/x$.

We focus on the degenerate state where the central frequencies for the signal and idler photons are identical, $\bar{\omega}_s = \bar{\omega}_i = \frac{1}{2}\bar{\omega}_p$. Taylor expansion of the wavenumber gives $k_j(\omega_j) \approx k_j(\bar{\omega}_j) + \Delta_j/v_j$, where $\Delta_j = \omega_j - \bar{\omega}_j$ and $v_j \equiv d\omega_j/dk_j$ is the group velocity of jth beam. Under the phase-matching condition $k_s(\bar{\omega}_s) + k_i(\bar{\omega}_i) - k_p(\bar{\omega}_p) = 0$, the JSA becomes

$$J(\Delta_s, \Delta_i) = \mathcal{N} \exp\left(-\frac{(\Delta_s + \Delta_i)^2}{4\sigma_p^2}\right) \mathrm{sinc}\left(\frac{1}{2}\bar{T}(\Delta_s + \Delta_i) + \frac{1}{2}(\Delta_s - \Delta_i)T_e\right) \quad (14)$$

where $T_e = \frac{1}{2}\left(\frac{L}{v_s} - \frac{L}{v_i}\right)$ is the entanglement time characterizing the difference between the arrival times of the photon pair and $\bar{T} = \frac{1}{2}\left(\frac{L}{v_s} + \frac{L}{v_i}\right) - \frac{L}{v_p}$ is the travel time difference between the biphoton and the pump inside the nonlinear crystal. The twin-photon JSAs for different entanglement times are shown in Figure 2. Each photon bandwidth is controlled by the entanglement time with shorter T_e leading to a broader bandwidth, whereas the sum frequencies of the signal and idler beams are narrowly distributed, independent of the bandwidth of individual photons. Useful information about the photon pair frequency entanglement can be obtained from the Hong−Ou−Mandel interference.[39]

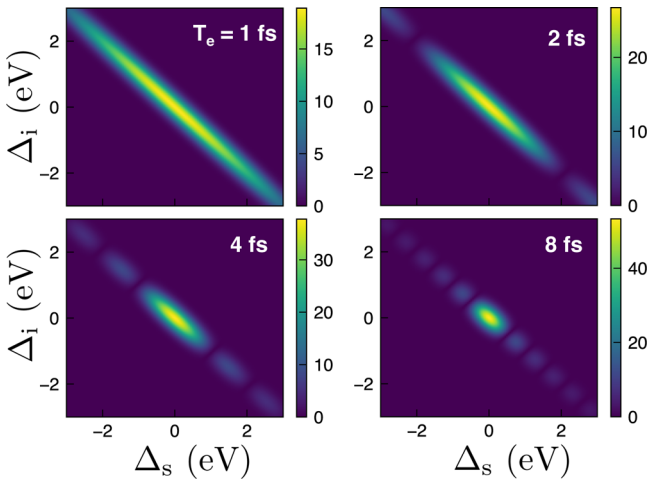

Figure 2. JSA $|J(\Delta_s,\Delta_i)|$ of the quantum light [eq 14] for different entanglement times T_e. Here, $\sigma_p = 0.2$ eV and $\bar{T} = 0$.

The two-photon detection amplitude is given by

$$\Phi_{is}(t_2, t_1) = \int_0^\infty\int_0^\infty d\omega_s\, d\omega_i \mathcal{E}(\omega_i)\mathcal{E}(\omega_s)\, e^{-i\omega_i t_2 - i\omega_s t_1} J(\omega_s, \omega_i) \quad (15)$$

https://doi.org/10.1021/acs.jctc.1c00949
J. Chem. Theory Comput. XXXX, XXX, XXX−XXX

Invoking the narrowband approximation $\mathcal{E}(\omega_j) \approx \mathcal{E}(\bar{\omega}_j)$, changing the variables to Δ_j, and extending the integration range to $(-\infty, \infty)$ yield

$$\Phi_{is}(t_2, t_1) = (2\pi)^2 \mathcal{E}(\bar{\omega}_i)\mathcal{E}(\bar{\omega}_s) \exp(-i\bar{\omega}_i t_2 - i\bar{\omega}_s t_1) J(t_1, t_2) \tag{16}$$

where $J(t_1, t_2) = \int\int_{-\infty}^{\infty} \frac{d\Delta_s\, d\Delta_i}{(2\pi)^2} J(\Delta_s, \Delta_i)\, e^{-i\Delta_i t_2 - i\Delta_s t_1}$ is the joint temporal amplitude of the twin photons. For $\bar{T} = 0$

$$J(t_1, t_2) = \sqrt{\sigma_p / T_e}\,(2\pi)^{-5/4}\, e^{-\sigma_p^2 (t_1+t_2)^2/4} \Pi\left(\frac{t_1 - t_2}{2T_e}\right) \tag{17}$$

where $\Pi(x) = 1$ for $|x| < 1/2$ and 0 otherwise.

Simulation Protocol Based on a Time Grid. Equation 11 suggests the following simulation protocol: we first sample (t_2,t_1) on a two-dimensional triangular grid, with t_2 ranging from t_0 to the final time t, and t_1 samples t_0 to t_2; for each (t_1,t_2), we compute the nuclear wave packet $\xi(t_2,t_1)$ by a wave packet dynamics solver. The final wave packet can then be obtained by summing over all $\xi(t_2,t_1)$.

The final nuclear wave packet eq 11 is simulated as follows (for brevity, we assume a single intermediate electronic state e):

1. Set the initial wave packet to $\chi_e(\mathbf{R}) = \mu_{eg}(\mathbf{R})\chi_0(\mathbf{R})$
2. Propagate the wave packet on the eth PES for time interval τ, leading to $\chi_e(\mathbf{R},\tau) = U_M(\tau)\mu_{eg}(\mathbf{R})\chi_0(\mathbf{R})$.
3. Using eq 15, perform the following integration to obtain an auxiliary wave packet $\zeta(\mathbf{R},t)$

$$\zeta(\mathbf{R}, \tau_2) = \int_0^{\tau_2} d\tau\, \Phi(\tau_2 + t_0, \tau_2 - \tau + t_0)\chi_e(\mathbf{R}, \tau) \tag{18}$$

4. For each $\tau_2 = t - t_0 - t_2$, apply the dipole operator to $\zeta(\mathbf{R},\tau_2)$ that brings the molecule to the final electronic state, $\mu_{fe}(\mathbf{R})\zeta(\mathbf{R},\tau_2)$, and propagate the wave packet for $t - t_0 - \tau_2$ on the final PES.

Summing up all possible τ_2 leads to

$$\chi_f(\mathbf{R}, T = t - t_0) = \int_0^T d\tau_2\, U_M(t - t_0 - \tau_2)\mu_{fe}(\mathbf{R})\zeta(\mathbf{R}, \tau_2) \tag{19}$$

The molecular propagator is computed using wave packet dynamics on a single PES.[40] The second-order split operator method is employed for adiabatic wave packet dynamics on a single PES $V_\alpha(\mathbf{R})$. A Trotter decomposition of the propagator is employed

$$U_\alpha(\delta t) = e^{-iV_\alpha \delta t/2}\, e^{-iT_n \delta t}\, e^{-iV_\alpha \delta t/2} + O((\delta t)^3) \tag{20}$$

for a short time interval δt and fast Fourier transform switching the wave function between the coordinate and momentum space.

RESULTS AND DISCUSSION

Simulations were carried out for a three-state displaced harmonic oscillator model with a single nuclear coordinate x and the corresponding momentum p. The PESs depicted in Figure 3 are given by

$$V_\alpha(x) = \frac{p^2}{2} + \frac{\omega_\alpha^2}{2}(x - d_\alpha)^2 + E_\alpha \tag{21}$$

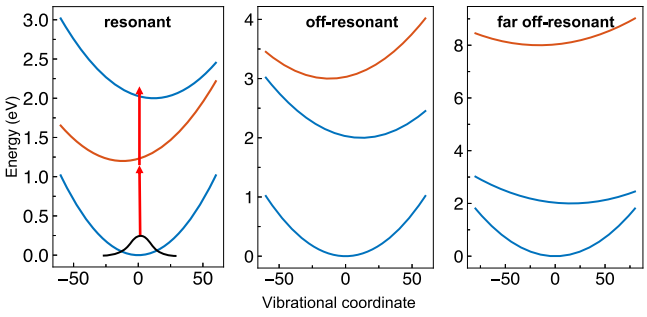

Figure 3. PESs of the displaced harmonic oscillator model corresponding to three different cases, where the intermediate electronic state is resonant, off-resonant, and far-off-resonant with the incoming photons. Correspondingly, E_e = 1, 3, and 8 eV.

where $\alpha = \{g, e, f\}$, referring to the ground, intermediate, and final electronic states, respectively; d_α is the displacement; and E_α is the zero-phonon line. By tuning the energy E_e, we cover three scenarios, whereby the intermediate PES is resonant, off-resonant, and far-off-resonant with respect to the incoming photons. Other parameters are $E_g = 0$, $E_f = 2$ eV, $d_g = 0$, and $d_e = -d_f = -10\ a_0$, $\omega_\alpha = 1000\ cm^{-1}$.

Sum-Over-States Expansion of the Molecular Response. We explore the variation of the electronic populations and wave packets with the entanglement time by employing the sum-over-states expression for the molecular response in the vibronic eigenstates of the molecular Hamiltonian H_M. Let $|\alpha\nu\rangle$ denote the vibronic states associated with αth electronic state with eigenenergies $\omega_{\alpha\nu}$; the free-molecular propagator and the interaction picture dipole operator are $U_M(t) = \sum_\alpha \sum_\nu e^{-i\omega_{\alpha\nu}t}|\alpha\nu\rangle\langle\alpha\nu|$ and $V^{(j)}(t) = \sum_{\beta\nu',\alpha\nu} V^{(j)}_{\beta\nu',\alpha\nu}\, e^{i\omega_{\beta\nu',\alpha\nu}t}|\beta\nu'\rangle\langle\alpha\nu|$, with $\omega_{\beta\nu',\alpha\nu} = \omega_{\beta\nu'} - \omega_{\alpha\nu}$.

Inserting these into eq 11 yields $|\chi_f(t)\rangle = \sum_\nu A_{f\nu,g0}(t)|f\nu\rangle$, where

$$T_{f\nu,g0}(t) = (2\pi)^2 \mathcal{E}(\bar{\omega}_i)\mathcal{E}(\bar{\omega}_s) \sum_{e,\nu'} \mu^{(i)}_{f\nu,e\nu'}\mu^{(s)}_{e\nu',g0} \int_{t_0}^{t} dt_2\, e^{i(\omega_{f\nu,e\nu'} - \bar{\omega}_i)t_2} \int_{t_0}^{t_2} dt_1\, e^{i(\omega_{e\nu',g0} - \bar{\omega}_s)t_1} J(t_1, t_2) \tag{22}$$

is the transition amplitude from the ground vibrational state in the ground electronic state PES $|g0\rangle$ to the vibronic state $|f\nu\rangle$. Using eq 17 and taking $t \to \infty$, $t_0 \to -\infty$ yield

$$A_{f\nu,g0} = (2\pi)^{3/4} \sqrt{\frac{\pi}{\sigma_p T_e}}\, \mathcal{E}(\bar{\omega}_i)\mathcal{E}(\bar{\omega}_s) \exp\left(-\frac{(\omega_{f\nu,g0} - \bar{\omega}_p)^2}{4\sigma_p^2}\right) \sum_{\nu'} \mu^{(i)}_{f\nu,e\nu'}\mu^{(s)}_{e\nu',g0} \frac{e^{i\Delta_{\nu'}T_e} - 1}{i\Delta_{\nu'}} + (s \leftrightarrow i) \tag{23}$$

where ν' runs over the vibrational eigenstates in eth PES, $\Delta_{\nu'} = \frac{1}{2}\omega_{f\nu,g0} - \omega_{e\nu',g0}$, and $\mu_{\beta\nu',\alpha\nu} = \langle\beta\nu'|\mu|\alpha\nu\rangle$ is the transition dipole moment between vibronic states.

Figure 4 depicts the two-photon-excited population as a function of the entanglement time. The largest excited population occurs for the resonant case (upper panel), as reflected in the detuning factor $1/\Delta_{\nu'}$ in eq 23. Interestingly, the population grows, roughly linearly, with T_e at short entanglement times. To rationalize this observation, we isolate

https://doi.org/10.1021/acs.jctc.1c00949
J. Chem. Theory Comput. XXXX, XXX, XXX−XXX

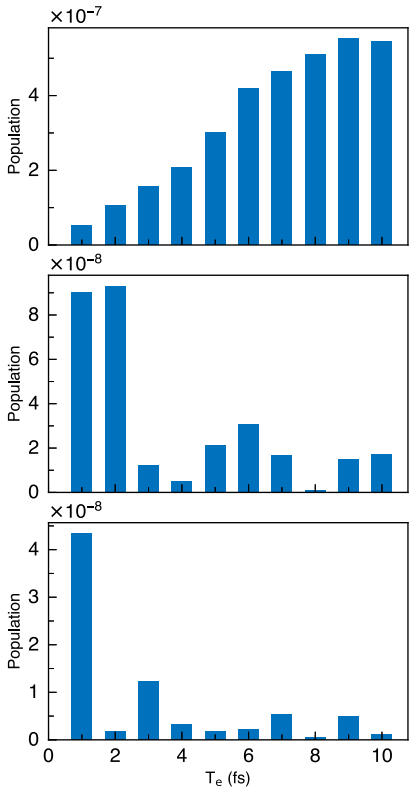

Figure 4. Dependence of the entangled two-photon-excited population on the entanglement time for (upper panel) the resonant intermediate state, (middle panel) off-resonant, and (lower panel) far-off-resonant. The parameters read $A = 1\ \mu m^2$, $n = 1$,$\bar{\omega}_p = 2.4$ eV, and $\sigma_p = 0.2$ eV.

the T_e-dependent factor in eq 23 $g(T_e) = \frac{1}{\sqrt{T_e}} \frac{e^{i\Delta_{\nu'} T_e} - 1}{i\Delta_{\nu'}}$, and we use $e^x \approx 1 + x$

$$P \propto |g(T_e)|^2 \approx T_e \tag{24}$$

Thus, for resonant intermediate states and short entanglement times, the two-photon-excited population grows linearly with T_e. After the first photon interacts with the molecules, transient population is built in the intermediate state. This population grows for a short period of time until the second photon arrives. The time window is bound by the entanglement time of the quantum light, whereas for classical light there is so such restriction. This linear increase only exists at very short entanglement times below $T_e = 10$ fs.

For off-resonant and far-off-resonant intermediate states (middle and lower panels of Figure 4), the two-photon-excited population shows a nonlinear dependence on the entanglement time. In both cases, the largest population occurs at short entanglement times, with the population for the off-resonant case larger than the far-off-resonant case, as expected.

Apart from controlling the electronic populations, the JSA may also be used to manipulate the nuclear wave packet. Figures 5−7 show the phase-space Wigner representation of the nuclear wave packets prepared by entangled light with various entanglement times at $t = 30$ fs ($t_0 = -20$ fs) for the resonant, off-resonant, and far-off-resonant cases. The Wigner spectrogram transforms the wave packet in the coordinate space as $\chi_W(x, p, t) = \int_{-\infty}^{\infty} dy\, \chi_f\left(x + \frac{y}{2}\right)\chi_f^*\left(x - \frac{y}{2}\right) e^{ipy}$. We see that the nuclear wave packet is most sensitive to the entanglement time in the off-resonant case, with minor variations otherwise. The nuclear wave packet depends on both the amplitude and phase of the transition amplitude to a vibronic state in the fth electronic state $A_{f\nu}$. For the resonant case, eq 24 implies that for short entanglement times, the

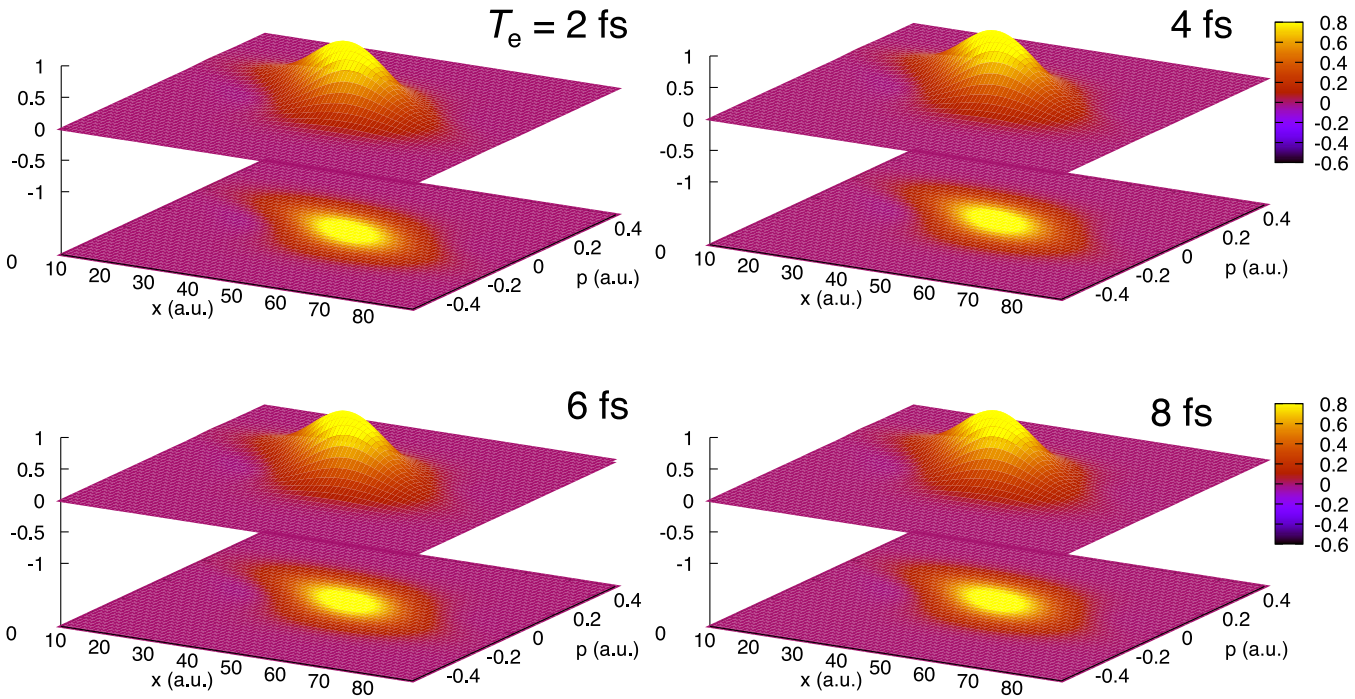

Figure 5. Phase-space representation of entangled two-photon-excited wave packets for the displaced harmonic oscillator model with a resonant intermediate electronic state for various entanglement times as indicated.

https://doi.org/10.1021/acs.jctc.1c00949
J. Chem. Theory Comput. XXXX, XXX, XXX−XXX

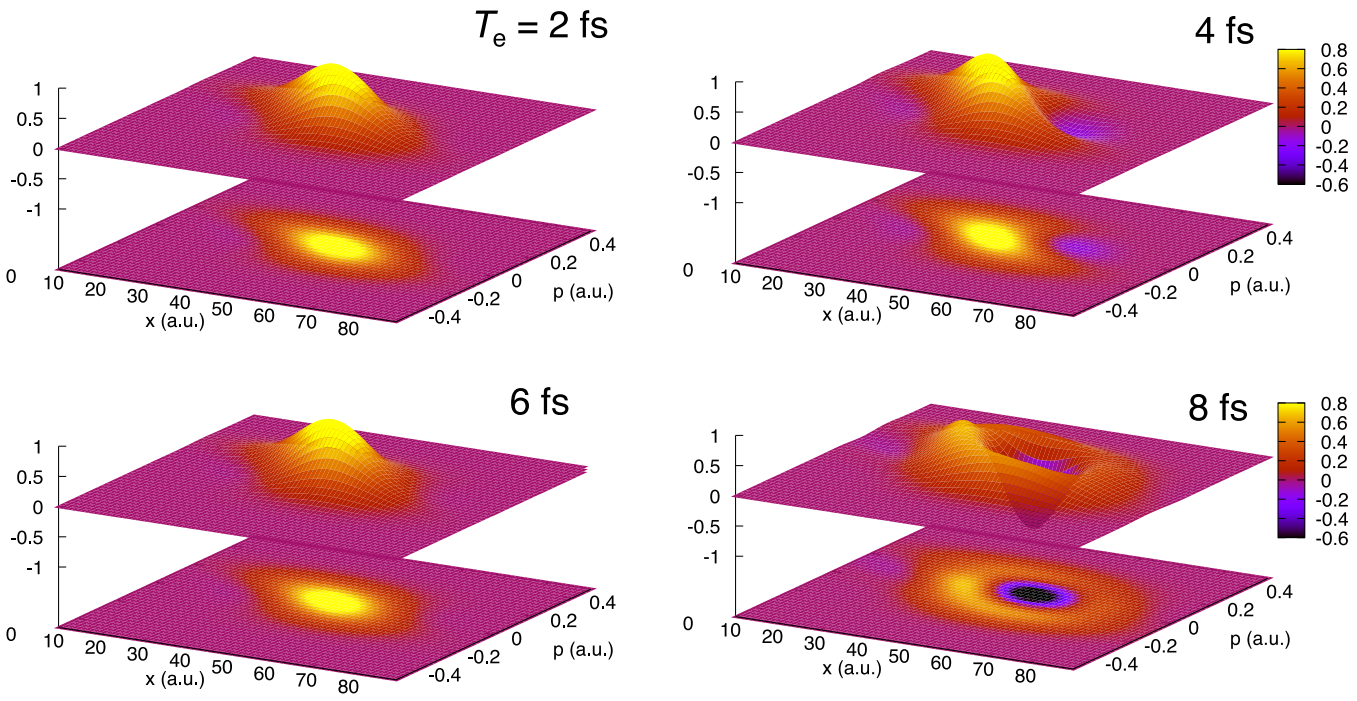

Figure 6. Phase-space representation of entangled two-photon-excited wave packets for the displaced harmonic oscillator model with an off-resonant intermediate electronic state for various entanglement times as indicated.

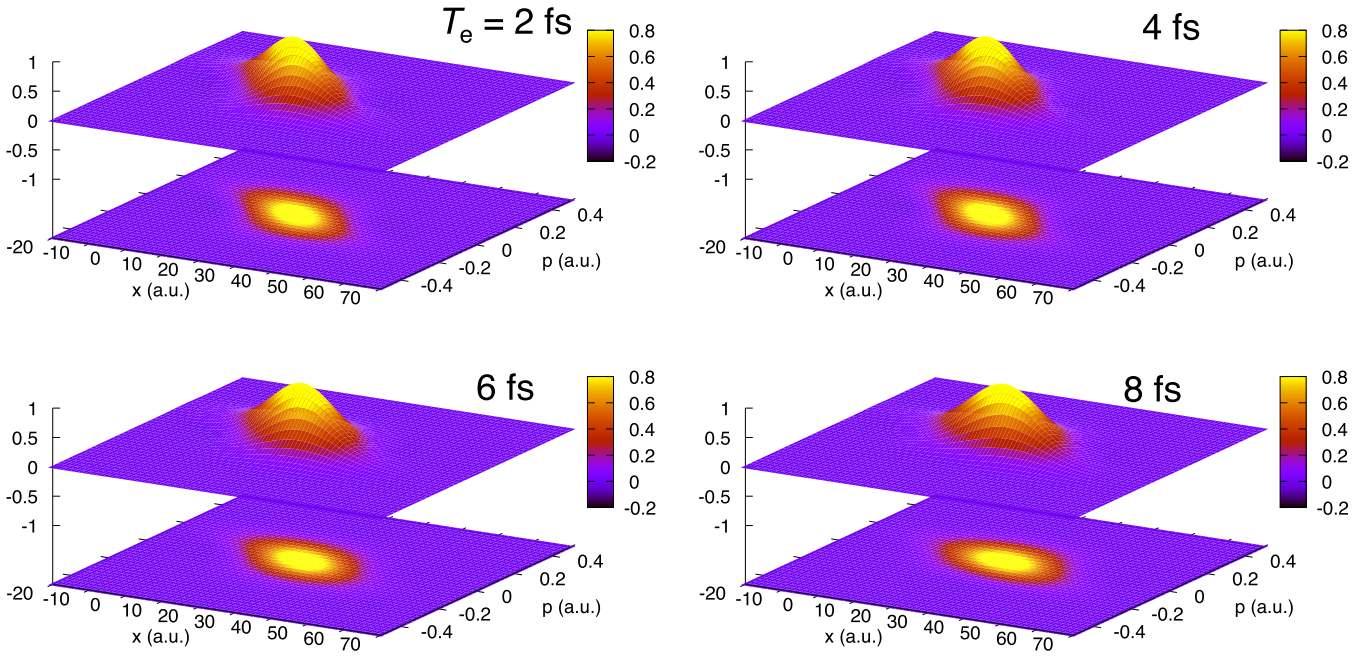

Figure 7. Phase-space representation of entangled two-photon-excited wave packets for the displaced harmonic oscillator model with a far-off-resonant intermediate electronic state for various entanglement times as indicated.

relative phase between the vibrational states in f-PES does not depend on T_e. For the off-resonant case, $g(T_e)$ will show an oscillatory behavior, and the relation between $A_{f\nu}$ and the vibrational state ν will strongly depend on T_e, thus leading to a considerable change in the wave packet.

Simulation Protocol Based on Schmidt Decomposition. Sampling the wave packets on the two-dimensional time grid is numerically expensive. We now present an alternative simulation protocol for the ETPA, which employs the Schmidt decomposition of the entangled light[41] and replaces the time grid sampling by a summation over Schmidt modes. The entangled light can be expanded in Schmidt modes. Each pair of modes leads to a transition amplitude, and summing over all contributing Schmidt modes leads to the final signal. The photon pair entanglement is then reflected in the quantum interference among the Schmidt modes.

Schmidt Decomposition of Quantum Light. With the Schmidt decomposition for the JSA,[41,42] $J(\omega_s, \omega_i) = \sum_n \sqrt{\lambda_n}\phi_n(\omega_s)\varphi_n(\omega_i)$, the two-photon wave function can then be expressed by

https://doi.org/10.1021/acs.jctc.1c00949
J. Chem. Theory Comput. XXXX, XXX, XXX−XXX

$$\Phi_{is}(t_2, t_1) = (2\pi)^2 \mathcal{E}(\bar{\omega}_i)\mathcal{E}(\bar{\omega}_s)\sum_n \sqrt{\lambda_n}\phi_n(t_1)\varphi_n(t_2) \tag{25}$$

where $\phi_n(t) = \int_{-\infty}^{\infty} \frac{d\omega}{2\pi}\phi_n(\omega)\, e^{i\omega t}$ and $\varphi_n(t)$ are the temporal modes, that is, Schmidt modes Fourier-transformed to the time domain; $\phi_n(\omega_s)$ and $\varphi_n(\omega_i)$ are the Schmidt modes that are, respectively, the eigenstates of the reduced density matrices of the signal and idler photons, with λ_n being the corresponding eigenvalues.

Inserting eq 25 into eq 11 leads to

$$\chi_f(\mathbf{R}, t) = (2\pi)^2 \mathcal{E}(\bar{\omega}_i)\mathcal{E}(\bar{\omega}_s)\sum_n \sqrt{\lambda_n}\kappa_n(\mathbf{R}, t)$$

$$\kappa_n(\mathbf{R}, t) \equiv \sum_e \int_{t_0}^{t} dt_2 \int_{t_0}^{t_2} dt_1\, U_f(t, t_2) V_{fe}^{\dagger}(\mathbf{R}) U_e(t_2, t_1) V_{eg}^{\dagger}(\mathbf{R})\chi_0(\mathbf{R})\phi_n(t_1)\varphi_n(t_2) \tag{26}$$

$\kappa_n(\mathbf{R},t)$ is the two-photon-excited nuclear wave packet with the nth pair of Schmidt modes. An important observation is that κ_n can be simply simulated by solving the time-dependent Schrödinger equation in the presence of two classical pulses, with the electric field $\mathcal{E}_s(t) = \phi_n(t)$, $\mathcal{E}_i(t) = \varphi_n(t)$. Therefore, instead of using a temporal grid, one can simply solve the time-dependent Schrödinger equation to compute the ETPA signal.

However, in classical two-photon absorption, there are additional second-order transition pathways corresponding to absorbing two photons from a single beam, which does not exist in quantum light. This becomes clear in the classical TPA expression

$$\chi_f(\mathbf{R}, t) \propto \int_{t_0}^{t} dt_2 \int_{t_0}^{t_2} dt_1 V_{fe}(t_2) V_{eg}(t_1)\chi_0(\mathbf{R}) (\mathcal{E}_s(t_2)\mathcal{E}_s(t_1) + \mathcal{E}_i(t_2)\mathcal{E}_s(t_1) + \mathcal{E}_s(t_2)\mathcal{E}_i(t_1) + \mathcal{E}_i(t_2)\mathcal{E}_i(t_1)) \tag{27}$$

where the additional terms are associated with $\mathcal{E}_i(t_2)\mathcal{E}_i(t_1)$ and $\mathcal{E}_s(t_2)\mathcal{E}_s(t_1)$. These have the same order as the desired ones, absorbing signal and idler photons together, and thus cannot be eliminated by weakening the field.

Selecting Pathways by Phase Cycling. To remove the undesired transition pathways, we can employ a phase-cycling protocol.[43,44] Phase cycling selectively extracts pathways by applying phases to the pulses

$$\mathcal{E}_j(t) \to e^{i\theta_j}\mathcal{E}_j(t) \tag{28}$$

for j = s, i. It exploits the fact that different pathways respond differently to the phase change.

A phase-cycling protocol that eliminates the two-photon transition pathways ss and ii is shown in Table 1.

Table 1. Phase-Cycling Protocol to Remove Additional Pathways[a]

	θ_s	θ_i	ss	ii	si	is
I	0	$\pi/2$	1	−1	i	i
II	$\pi/2$	0	−1	1	i	i

[a]The final signal $S = \frac{1}{2i}(S_I + S_{II})$. The four pathways are labeled by the signal (s) and idler (i) photons interacting with the molecule in the given order.

This protocol with Schmidt modes can be very efficient if the entangled light can be described by a limited number of Schmidt modes.[45]

CONCLUSIONS

We have presented a computational protocol for the ETPA signal in molecules which takes the nuclear quantum dynamics into account. It involves summing over all transition pathways determined by two light−matter interaction times. This development, going beyond the two-photon absorption rate,[46] is valid for resonant intermediate states and provides not only information of the populations but also of coherences. Using a displaced harmonic oscillator model, we have demonstrated how entangled light can be used to manipulate the two-photon excitation process. Both electronic populations and nuclear wave packets strongly depend on the entanglement time. This protocol applies to any JSA of the entangled light and thus can be applied for various sources of quantum light from, for example, cascaded emission as well. We have also outlined an alternative protocol based on the Schmidt decomposition of the entangled light, which can be very efficient if the entangled light can be described by a limited number of Schmidt modes (weak entanglement).

Our protocols allow the simulation of quantum light spectroscopy of complex molecular systems fully accounting for the coupled electronic−nuclear−photonic motion. Future perspectives include incorporating more vibrational modes of polyatomic molecules and solvent environment that can introduce electronic and vibrational decoherence.[47−49] Advances in pulse shaping techniques may allow a complete control of the JSA by varying the parameters other than entanglement time.[35]

AUTHOR INFORMATION

Corresponding Authors

Bing Gu − *Department of Chemistry & Department of Physics and Astronomy, University of California Irvine, Irvine, California 92697, United States;* orcid.org/0000-0002-5787-3334; Email: bingg@uci.edu

Shaul Mukamel − *Department of Chemistry & Department of Physics and Astronomy, University of California Irvine, Irvine, California 92697, United States;* orcid.org/0000-0002-6015-3135; Email: smukamel@uci.edu

Author

Daniel Keefer − *Department of Chemistry & Department of Physics and Astronomy, University of California Irvine, Irvine, California 92697, United States;* orcid.org/0000-0001-5941-5567

Complete contact information is available at: https://pubs.acs.org/10.1021/acs.jctc.1c00949

Notes

The authors declare no competing financial interest.

ACKNOWLEDGMENTS

The authors thank Dr. Feng Chen for inspiring discussions.The support of the National Science Foundation Grant CHE-1953045 and of the U.S. Department of Energy, Office of Science, Office of Basic Energy Sciences under award DE-SC0020168 is gratefully acknowledged. B.G. was supported by the DOE grant. D.K. acknowledges support from the

https://doi.org/10.1021/acs.jctc.1c00949
J. Chem. Theory Comput. XXXX, XXX, XXX−XXX

Alexander von Humboldt Foundation through the Feodor Lynen program.

REFERENCES

(1) Mukamel, S.; et al. Roadmap on Quantum Light Spectroscopy. *J. Phys. B: At., Mol. Opt. Phys.* **2020**, *53*, 072002.
(2) Dorfman, K. E.; Schlawin, F.; Mukamel, S. Nonlinear Optical Signals and Spectroscopy with Quantum Light. *Rev. Mod. Phys.* **2016**, *88*, 045008.
(3) Li, F.; Li, T.; Scully, M. O.; Agarwal, G. S. Quantum Advantage with Seeded Squeezed Light for Absorption Measurement. *Phys. Rev. Appl.* **2021**, *15*, 044030.
(4) Roslyak, O.; Mukamel, S. A Unified Description of Sum Frequency Generation, Parametric down Conversion and Two-Photon Fluorescence. *Mol. Phys.* **2009**, *107*, 265−280.
(5) Chen, F.; Mukamel, S. Vibrational Hyper-Raman Molecular Spectroscopy with Entangled Photons. *ACS Photonics* **2021**, *8*, 2722−2727.
(6) Cao, J.; Che, J.; Wilson, K. R. Intrapulse Dynamical Effects in Multiphoton Processes: Theoretical Analysis. *J. Phys. Chem. A* **1998**, *102*, 4284−4290.
(7) Hong, C. K.; Ou, Z. Y.; Mandel, L. Measurement of Subpicosecond Time Intervals between Two Photons by Interference. *Phys. Rev. Lett.* **1987**, *59*, 2044−2046.
(8) Eshun, A.; Gu, B.; Varnavski, O.; Asban, S.; Dorfman, K. E.; Mukamel, S.; Goodson, T. Investigations of Molecular Optical Properties Using Quantum Light and Hong-Ou-Mandel Interferometry. *J. Am. Chem. Soc.* **2021**, *143*, 9070−9081.
(9) Kalashnikov, D. A.; Melik-Gaykazyan, E. V.; Kalachev, A. A.; Yu, Y. F.; Kuznetsov, A. I.; Krivitsky, L. A. Quantum Interference in the Presence of a Resonant Medium. *Sci. Rep.* **2017**, *7*, 11444.
(10) Dorfman, K. E.; Asban, S.; Gu, B.; Mukamel, S. Hong-Ou-Mandel Interferometry and Spectroscopy Using Entangled Photons. *Commun. Phys.* **2021**, *4*, 49.
(11) Landes, T.; Raymer, M. G.; Allgaier, M.; Merkouche, S.; Smith, B. J.; Marcus, A. H.; Merkouche, S.; Merkouche, S.; Smith, B. J.; Smith, B. J.; Marcus, A. H.; Marcus, A. H. Quantifying the Enhancement of Two-Photon Absorption Due to Spectral-Temporal Entanglement. *Opt. Express* **2021**, *29*, 20022−20033.
(12) Raymer, M. G.; Marcus, A. H.; Widom, J. R.; Vitullo, D. L. P. Entangled Photon-Pair Two-Dimensional Fluorescence Spectroscopy (EPP-2DFS). *J. Phys. Chem. B* **2013**, *117*, 15559−15575.
(13) Oka, H. Entangled Two-Photon Absorption Spectroscopy for Optically Forbidden Transition Detection. *J. Chem. Phys.* **2020**, *152*, 044106.
(14) Terenziani, F.; Katan, C.; Badaeva, E.; Tretiak, S.; Blanchard-Desce, M. Enhanced Two-Photon Absorption of Organic Chromophores: Theoretical and Experimental Assessments. *Adv. Mater.* **2008**, *20*, 4641−4678.
(15) Mollow, B. Two-Photon Absorption and Field Correlation Functions. *Phys. Rev.* **1968**, *175*, 1555−1563.
(16) Schlawin, F.; Dorfman, K. E.; Mukamel, S. Entangled Two-Photon Absorption Spectroscopy. *Acc. Chem. Res.* **2018**, *51*, 2207−2214.
(17) Li, T.; Li, F.; Altuzarra, C.; Classen, A.; Agarwal, G. S. Squeezed Light Induced Two-Photon Absorption Fluorescence of Fluorescein Biomarkers. *Appl. Phys. Lett.* **2020**, *116*, 254001.
(18) Eshun, A.; Cai, Z.; Awies, M.; Yu, L.; Goodson, T. Investigations of Thienoacene Molecules for Classical and Entangled Two-Photon Absorption. *J. Phys. Chem. A* **2018**, *122*, 8167−8182.
(19) Parzuchowski, K. M.; Mikhaylov, A.; Mazurek, M. D.; Wilson, R. N.; Lum, D. J.; Gerrits, T.; Camp, C. H., Jr.; Stevens, M. J.; Jimenez, R. Setting Bounds on Two-Photon Absorption Cross-Sections in Common Fluorophores with Entangled Photon Pair Excitation. *Phys. Rev. Appl.* **2021**, *15*, 044012.
(20) Oka, H. Highly-Efficient Entangled Two-Photon Absorption with the Assistance of Plasmon Nanoantenna. *J. Phys. B: At., Mol. Opt. Phys.* **2015**, *48*, 115503.
(21) Gu, B.; Mukamel, S. Manipulating Two-Photon-Absorption of Cavity Polaritons by Entangled Light. *J. Phys. Chem. Lett.* **2020**, *11*, 8177−8182.
(22) Gea-Banacloche, J. Two-Photon Absorption of Nonclassical Light. *Phys. Rev. Lett.* **1989**, *62*, 1603−1606.
(23) Guzman, A. R.; Harpham, M. R.; Süzer, Ö.; Haley, M. M.; Goodson, T. G. Spatial Control of Entangled Two-Photon Absorption with Organic Chromophores. *J. Am. Chem. Soc.* **2010**, *132*, 7840−7841.
(24) Varnavski, O.; Goodson, T. Two-Photon Fluorescence Microscopy at Extremely Low Excitation Intensity: The Power of Quantum Correlations. *J. Am. Chem. Soc.* **2020**, *142*, 12966−12975.
(25) Szoke, S.; Liu, H.; Hickam, B. P.; He, M.; Cushing, S. K. Entangled light-matter interactions and spectroscopy. *J. Mater. Chem. C* **2020**, *8*, 10732−10741.
(26) Fei, H.-B.; Jost, B. M.; Popescu, S.; Saleh, B. E. A.; Teich, M. C. Entanglement-Induced Two-Photon Transparency. *Phys. Rev. Lett.* **1997**, *78*, 1679−1682.
(27) Tabakaev, D.; Montagnese, M.; Haack, G.; Bonacina, L.; Wolf, J.-P.; Zbinden, H.; Thew, R. T. Energy-Time-Entangled Two-Photon Molecular Absorption. *Phys. Rev. A* **2021**, *103*, 033701.
(28) Lee, D.-I.; Goodson, T. Entangled Photon Absorption in an Organic Porphyrin Dendrimer. *J. Phys. Chem. B* **2006**, *110*, 25582−25585.
(29) Javanainen, J.; Gould, P. L. Linear Intensity Dependence of a Two-Photon Transition Rate. *Phys. Rev. A: At., Mol., Opt. Phys.* **1990**, *41*, 5088−5091.
(30) Couteau, C. Spontaneous Parametric Down-Conversion. *Contemp. Phys.* **2018**, *59*, 291−304.
(31) Rubin, M. H.; Klyshko, D. N.; Shih, Y. H.; Sergienko, A. V. Theory of Two-Photon Entanglement in Type-II Optical Parametric down-Conversion. *Phys. Rev. A: At., Mol., Opt. Phys.* **1994**, *50*, 5122−5133.
(32) Rubin, M. H. Transverse Correlation in Optical Spontaneous Parametric Down-Conversion. *Phys. Rev. A: At., Mol., Opt. Phys.* **1996**, *54*, 5349−5360.
(33) Keller, T. E.; Rubin, M. H. Theory of Two-Photon Entanglement for Spontaneous Parametric down-Conversion Driven by a Narrow Pump Pulse. *Phys. Rev. A: At., Mol., Opt. Phys.* **1997**, *56*, 1534−1541.
(34) Muthukrishnan, A.; Agarwal, G. S.; Scully, M. O. Inducing Disallowed Two-Atom Transitions with Temporally Entangled Photons. *Phys. Rev. Lett.* **2004**, *93*, 093002.
(35) Schlawin, F. Entangled Photon Spectroscopy. *J. Phys. B: At., Mol. Opt. Phys.* **2017**, *50*, 203001.
(36) Mukamel, S. *Principles of Nonlinear Optical Spectroscopy*; Oxford University Press, 1995.
(37) Glauber, R. J. The Quantum Theory of Optical Coherence. *Phys. Rev.* **1963**, *130*, 2529−2539.
(38) Walborn, S. P.; Monken, C. H.; Pádua, S.; Souto Ribeiro, P. H. Spatial Correlations in Parametric Down-Conversion. *Phys. Rep.* **2010**, *495*, 87−139.
(39) Barbieri, M.; Roccia, E.; Mancino, L.; Sbroscia, M.; Gianani, I.; Sciarrino, F. What Hong-Ou-Mandel Interference Says on Two-Photon Frequency Entanglement. *Sci. Rep.* **2017**, *7*, 7247.
(40) Kosloff, R. Time-Dependent Quantum-Mechanical Methods for Molecular Dynamics. *J. Chem. Phys.* **1988**, *92*, 2087−2100.
(41) Law, C. K.; Eberly, J. H. Analysis and Interpretation of High Transverse Entanglement in Optical Parametric Down Conversion. *Phys. Rev. Lett.* **2004**, *92*, 127903.
(42) Raymer, M. G.; Walmsley, I. A. Temporal Modes in Quantum Optics: Then and Now. *Phys. Scr.* **2020**, *95*, 064002.
(43) Tan, H.-S. Theory and Phase-Cycling Scheme Selection Principles of Collinear Phase Coherent Multi-Dimensional Optical Spectroscopy. *J. Chem. Phys.* **2008**, *129*, 124501.
(44) Cho, D.; Rouxel, J. R.; Kowalewski, M.; Saurabh, P.; Lee, J. Y.; Mukamel, S. Phase Cycling RT-TDDFT Simulation Protocol for Nonlinear XUV and X-Ray Molecular Spectroscopy. *J. Phys. Chem. Lett.* **2018**, *9*, 1072−1078.

https://doi.org/10.1021/acs.jctc.1c00949
J. Chem. Theory Comput. XXXX, XXX, XXX−XXX

(45) Eberly, J. H. Schmidt Analysis of Pure-State Entanglement. *Laser Phys.* **2006**, *16*, 921−926.
(46) Craig, D. P.; Thirunamachandran, T. *Molecular Quantum Electrodynamics: An Introduction to Radiation-Molecule Interactions*; Courier Corporation, 1998.
(47) Gu, B.; Franco, I. Quantifying Early Time Quantum Decoherence Dynamics through Fluctuations. *J. Phys. Chem. Lett.* **2017**, *8*, 4289−4294.
(48) Nitzan, A. *Chemical Dynamics in Condensed Phases: Relaxation, Transfer and Reactions in Condensed Molecular Systems*; Oxford University Press, 2006.
(49) Gu, B.; Franco, I. Generalized Theory for the Timescale of Molecular Electronic Decoherence in the Condensed Phase. *J. Phys. Chem. Lett.* **2018**, *9* (4), 773−778.

https://doi.org/10.1021/acs.jctc.1c00949
J. Chem. Theory Comput. XXXX, XXX, XXX−XXX